


What determines the H I gas content in galaxies?:
morphological dependence of the H I gas fraction across M_* - SFR plane

SHIGIERU V. NAMIKI ^{1,2} YUSEI KOYAMA,^{1,2} SHUHEI, KOYAMA,³ TAKUJI YAMASHITA,⁴ MASAO HAYASHI,⁴
MARTHA P. HAYNES,⁵ RHYTHM SHIMAKAWA,² AND MASATO ONODERA^{1,2}

¹*The Graduate University for Advanced Studies, SOKENDAI, 2-21-1 Osawa, Mitaka, Tokyo, 181-8588, Japan*

²*Subaru Telescope, National Astronomical Observatory of Japan, National Institutes of Natural Sciences, 650 North A'ohoku Place, Hilo, HI 96720, USA*

³*Institute of Astronomy, Graduate School of Science, University of Tokyo, 2-21-1 Osawa, Mitaka, Tokyo 181-0015, Japan*

⁴*National Astronomical Observatory of Japan, National Institutes of Natural Sciences, 2-21-1 Osawa, Mitaka, Tokyo 181-8588, Japan*

⁵*Cornell Center for Astrophysics and Planetary Science, Space Sciences Building, Cornell University, Ithaca, NY 14853 USA*

(Received; Revised; Accepted May 7, 2021)

Submitted to ApJ

ABSTRACT

We perform a stacking analysis of the H I spectra from the Arecibo Legacy Fast ALFA (ALFALFA) survey for optically-selected local galaxies from the Sloan Digital Sky Survey (SDSS) to study the average gas fraction of galaxies at fixed stellar mass (M_*) and star formation rate (SFR). We first confirm that the average gas fraction strongly depends on the stellar mass and SFR of host galaxies; massive galaxies tend to have a lower gas fraction, and actively star-forming galaxies show higher gas fraction, which is consistent with many previous studies. Then we investigate the morphological dependence of the H I gas mass fraction at fixed M_* and SFR to minimize the effects of these parameters. We

Поставленная цель:

Уточнить связь содержания HI с морфологией, массой звездного населения и SFR галактик

Связь MHI с M^* и SFR хорошо известна. Какая связь с морфологией галактик, где есть SF?

В разных работах по разному определяется морфологический тип и по разному относят галактику к пассивным или активным.

Как отделить поздние типы от ранних? Либо по распределению яркости, либо по внешнему виду.

Другая проблема - селекция в сторону галактик наиболее богатых HI.

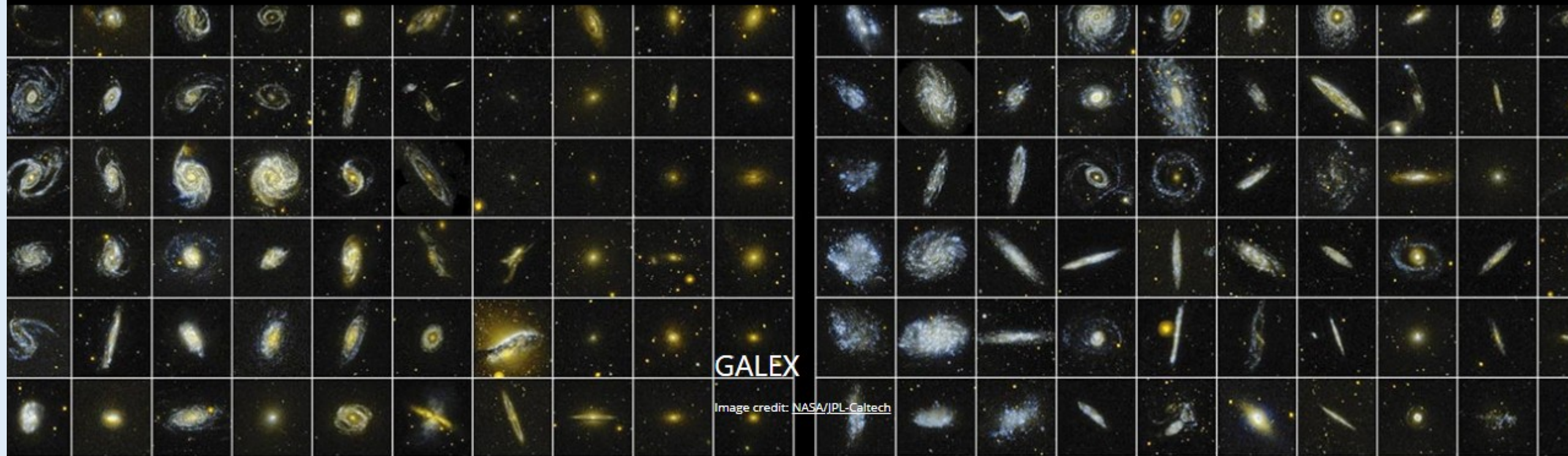
- In our study, we carry out a comprehensive analysis by using the multiple morphological indicators (индекс Серсика, C-индекс (R90/R50), smoothness(galactic Zoo project), разделяя при этом галактики по M^* и SFR.

Выборка – каталог GSWLC-2 (GALEX-SDSS-WISE LEGACY)(Salim et al 2018), где M^* и SFR оценивались для 230 000 SDSS-галактик с использованием GALEX и WISE.

We then cross-matched the GSWLC2 catalog with the MPA-JHU catalog (Abazajian et al. 2009) of SDSS DR7 to obtain the spectroscopic redshift of each target. We then select 32,717 galaxies (with $0.01 < z < 0.05$) located within the ALFALFA H I 21 cm line survey footprint.

CONTACT

RELEVANT LINKS



GALEX

Image credit: [NASA/JPL-Caltech](#)

GSWLC

GALEX-SDSS-WISE LEGACY CATALOG

Salim, Lee, Janowiecki, da Cunha, Dickinson, Boquien, Burgarella, Salzer and Charlot

GSWLC contains physical properties of ~700,000 galaxies with SDSS redshifts below 0.3 ($0.01 < z < 0.30$) and magnitude < 18 .

- We cross-matched the GSWLC2 catalog with the MPA-JHU catalog (Abazajian et al. 2009) based on SDSS DR7 to obtain the spectroscopic redshift of each target. We then select **32,717 galaxies** (with $0.01 < z < 0.05$) located within the ALFALFA H I 21 cm line survey footprint.
- HI - по каталогу ASLFALFA
- In the following analysis, we restrict the sample to galaxies with M^* and SFR range of $9.0 < \log M^* < 12.0$ and $-2.0 < \log \text{SFR} < 2.0$.
- Исключались галактики с компаньонами в пределах 4'.
- Исключались галактики с AGN (по BPT-диаграмме).
- The remaining **10,887 galaxies** are our parent 'star-forming' galaxy sample.

Go to the latest [Data Release](#).

Datasets

Imaging Data

Optical
Spectra

APOGEE
IR Spectra

MaStar
Library

MaNGA
IFU Spectra

Algorithms

Help

Tutorials

MPA-JHU Stellar Masses

Guinevere Kauffmann

GALAXY

Legacy

DR8

Type: Scientific Analysis Catalog

Location on SAS: <https://data.sdss.org/sas/dr8/sdss/spectro/redux/>

This VAC is described in full on [this web page](#).

The Max Planck for Astrophysics (MPA) and Johns Hopkins University (JHU) groups provide galaxy properties for all DR8 galaxy spectra, using the Galspec product, based on the methods of [Brinchmann et al. \(2004\)](#), [Kauffmann et al. \(2003\)](#), and [Tremonti et al. \(2004\)](#). The catalog includes emission lines and derived galaxy parameters, such as BPT (Baldwin, Phillips & Terlevich) properties, stellar mass, nebular oxygen abundance, and (specific) star formation rate. This catalog was deprecated in DR12 in favor of the [Wisconsin](#), [Portsmouth](#), and [Granada](#) team analyses of the same data, but are provided for comparison with the other galaxy property measurements listed here.

[SDSS](#) / [Value Added Catalogs](#) / MPA-JHU Stellar Masses

Overview

Tools

Value Added Catalogs

SDSS Supernovae

Bulk Downloads

Data Volume

System Status

VAC Filters



ENG

12:03

17.05.2021



21

ЧТО НОВОГО В МЕТОДИКЕ ОЦЕНКИ МАССЫ

- In short, instead of fitting an SED that includes both stellar (UV/optical) and dust (IR) SEDs, we perform UV/optical SED fitting that includes constraints on the dust emission directly from the total IR luminosity, i.e., the IR luminosity is treated as a “flux” point.

- Для уменьшения эффектов селекции при оценке МНІ использовалось сложение спектров НІ (stacking)

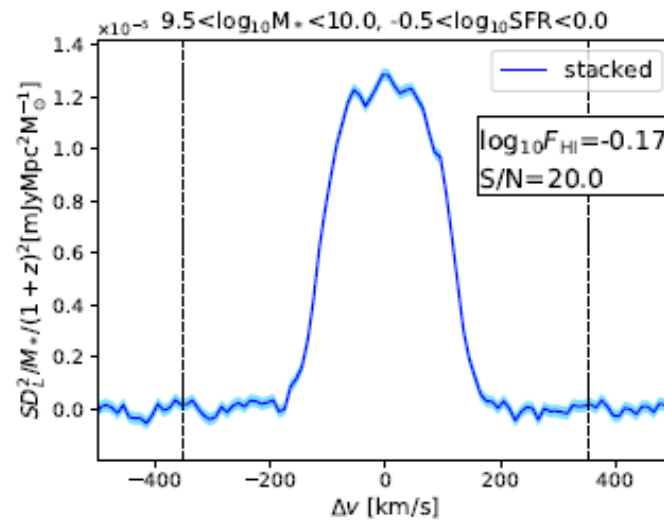


Figure 1. An example of the stacked H I spectra obtained in Sec. 2.2. The light-blue region shows the error in each velocity bin derived from the *rms* of individual spectra. Vertical dashed lines are shown at ± 350 km/s, between which the flux is summed up to calculate the gas fraction (F_{HI} , see Sec. 2.1).

- In our study, we divide our sample into small bins on the M^* -SFR plane ($\Delta M^* = \Delta \text{SFR} = 0.5$ dex). The galaxies in each bin are further divided by their morphology with three morphological indicators; Sersic n , C-index, and the visual smoothness. Our study revealed that visually smooth galaxies have lower gas fraction than non-smooth galaxies at fixed stellar mass and SFR.
- Such a morphological trend is not observed when we use C-index

Our results suggest that galaxy morphologies defined by Sérsic n and C -index are not identical to the class made by human eyes. We note that we are not discussing which is the best indicator of galaxy morphologies.

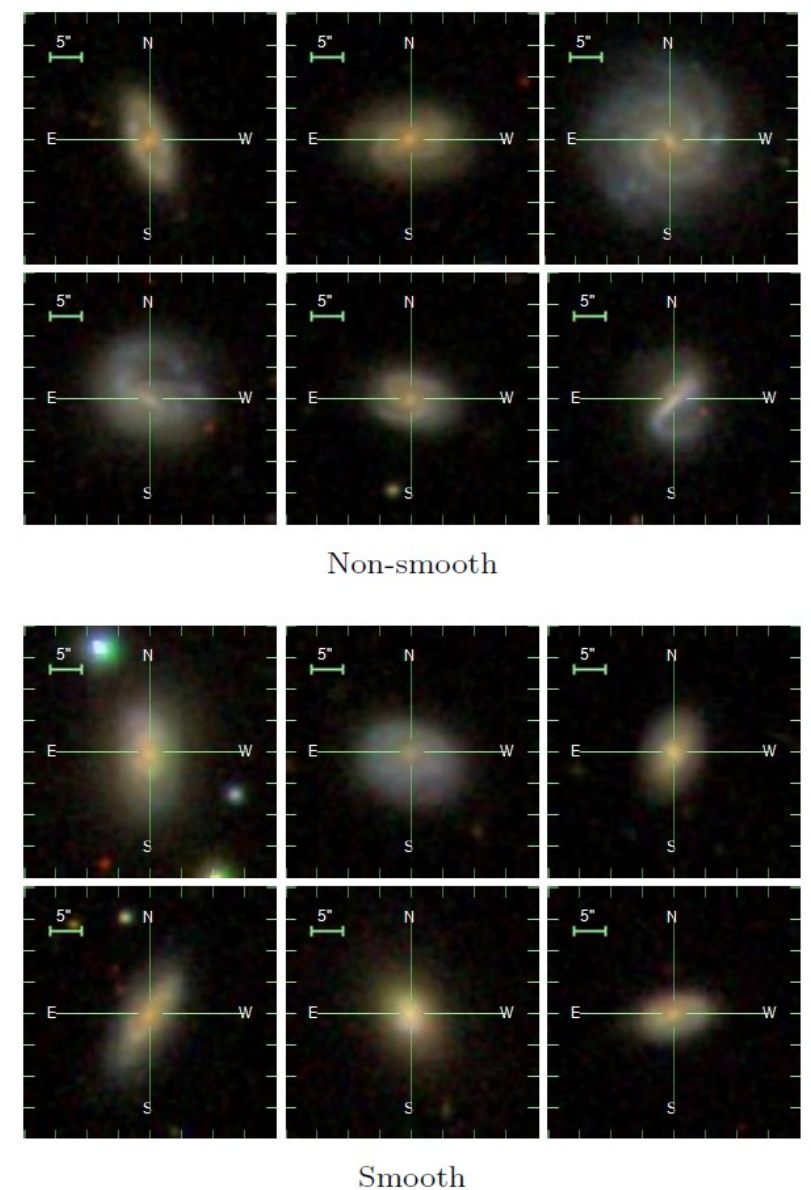


Figure 9. Examples of optical images of non-smooth (upper 6 panels) and smooth galaxies (lower 6 panels) from SDSS DR12. We note that all these galaxies listed here have fixed stellar mass, SFR , Sérsic n , and C -index ($10.0 < \log_{10} M_* < 10.5$, $0.0 < \log_{10} SFR < 0.5$, $1.0 < n < 1.5$, $2.0 < C < 2.5$).

Указано число галактик

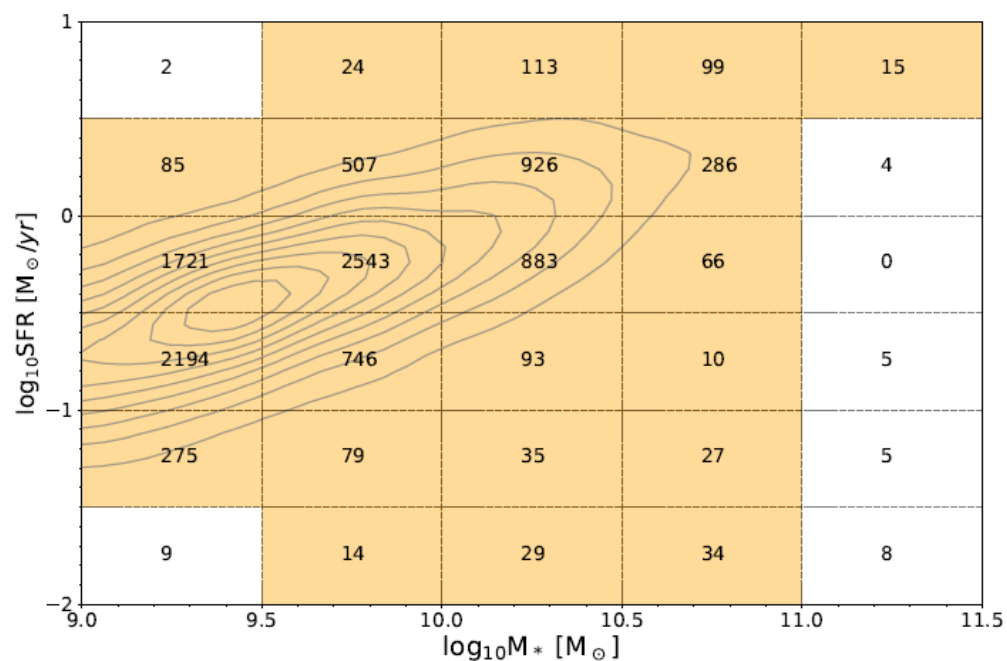


Figure 2. The M_* - SFR diagram to show the distribution of all our sample (grey contours) and the number of galaxies used for H I stacking at each (M_*, SFR) bin. The grid size indicates $\Delta M_* = \Delta SFR = 0.5$ dex (see Sec. 2.2 for details). Orange shaded bins are used for the stacking ($N \geq 10$).

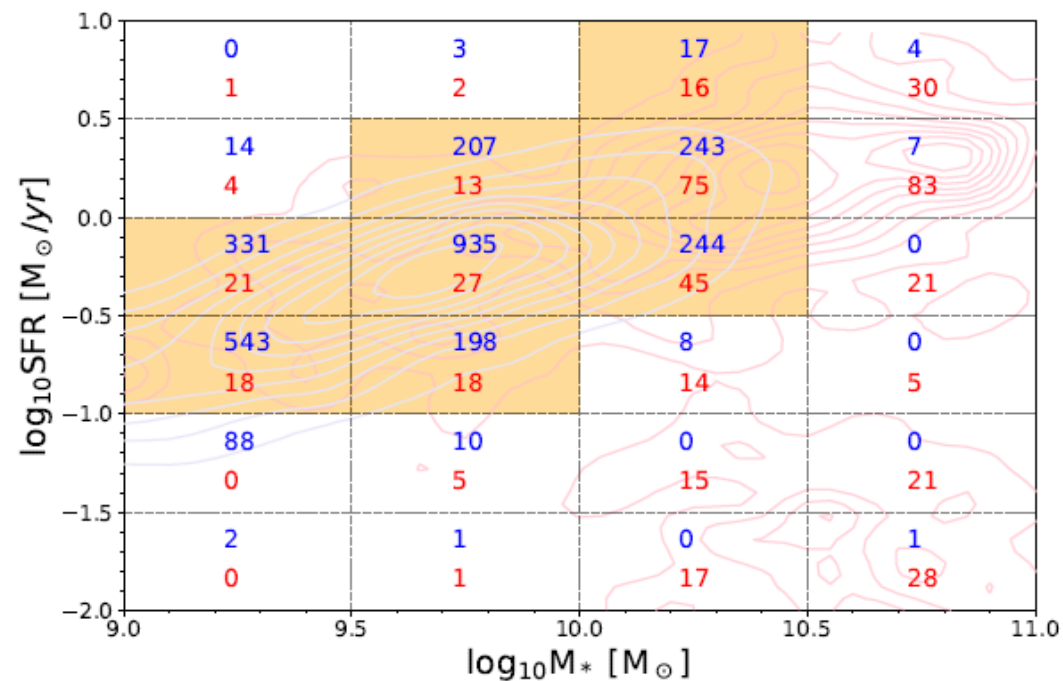


Figure 4. Same figure as Figure 2 but for late-type (blue) and early-type (red) galaxies divided by the Sérsic n . Blue and red contours show the distribution of late-type and early-type galaxies on this plane, respectively. Here we normalize the contours based on the total number of each population.

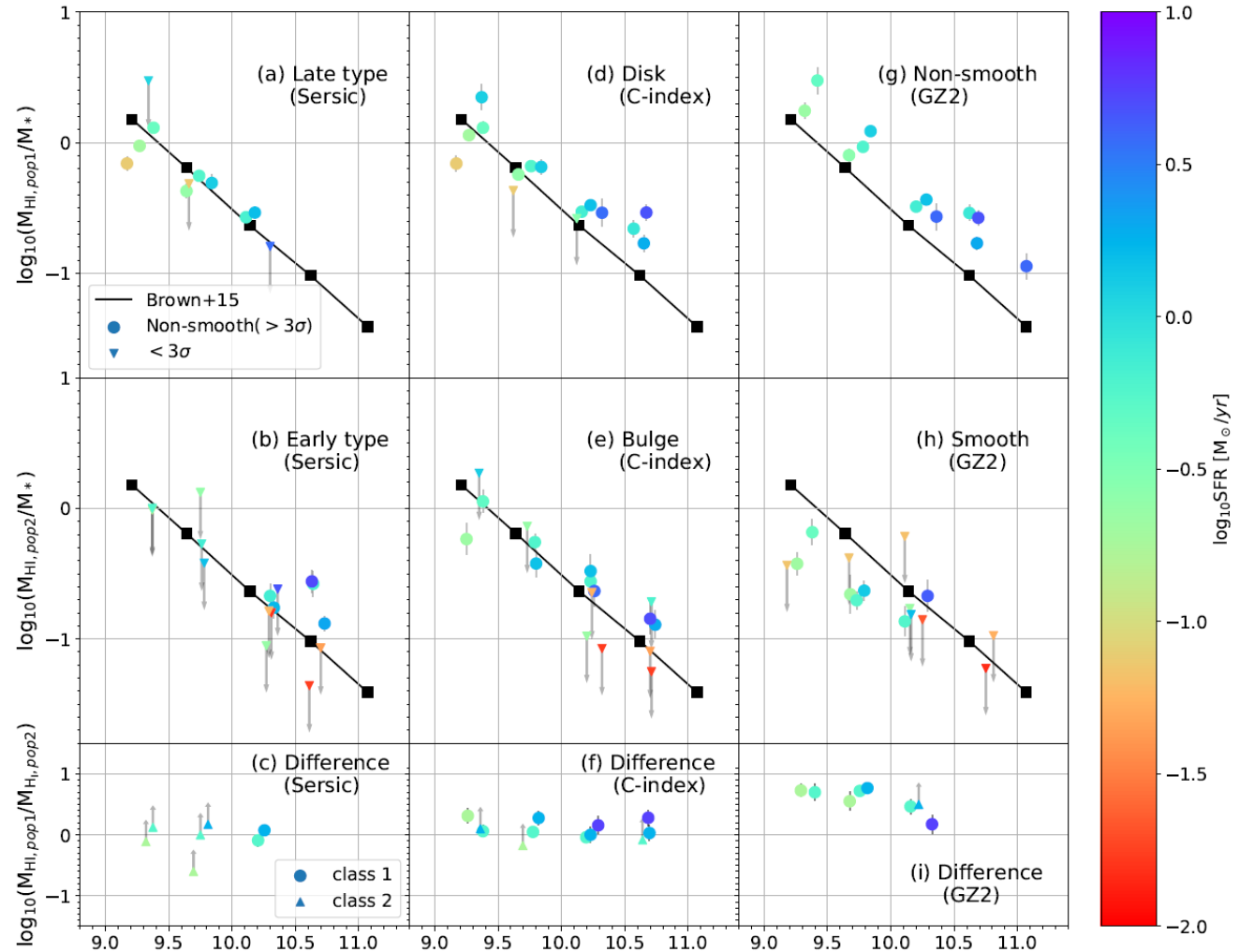


Figure 5. The result of our stacking analysis when we divide our sample by Sérsic n (left), C-index (middle), and visual smoothness (right). The top panels (a)/(d)/(g) show the relation between the stellar mass and the average H I gas fraction of late-type/disk/non-smooth populations, respectively. The second row (b)/(e)/(h) is the same as the upper panels but for early-type/bulge/smooth galaxies. The meanings of the large circles and inverted triangles in the top and second row are the same as the right panel of Figure 3. The panels (c)/(f)/(i) show the difference in the amount of H I gas between the above two populations as a function of their stellar mass. The meaning of each symbol is summarized in Sec. 3.1. Colors indicate the median SFR of each subsample. The gray error bars are also derived by the Bootstrap method (see Sec.2.1). The black squares connected by the solid line show the scaling relation from Brown et al. (2015) (same as Figure 3).

Выводы

- Our study revealed that, at fixed stellar mass and SFR, H I gas mass fraction (FHI) does not significantly depend on their morphologies when we use C-index for morphological classification, while we do find a significant morphological difference (0.7 dex) when we use visual smoothness as a morphological indicator. **The visual smoothness can better distinguish gas-rich and gas-poor populations at fixed stellar mass and SFR.**
- Smooth galaxies tend to have significantly lower gas fraction than non-smooth galaxies, and we find that there are six bins where both non-smooth and smooth galaxies are detected at $S/N(\text{FHI}) > 3$. There is a significant difference in H I gas fraction between the smooth and non-smooth galaxies at fixed stellar mass and SFR in the range of $9.0 < \log M < 10.5$. **This is the main result of our paper.**
- Considering the fact that the amount of molecular hydrogen is almost constant (Catinella et al. 2018; Koyama et al. 2019), our result suggests **that non-smooth galaxies have a larger amount of H I that is not involved in the star-formation** than smooth galaxies, even at the same stellar mass and SFR.

От себя:

Структурность (smoothness) отражает неоднородное (несимметричное) распределение молодых объектов в диске. Чем выше содержание газа, тем при тех же темпах S_f меньше smoothness (спиральные ветви, бар?)